Journal of the Nigerian Association of Mathematical Physics, Volume 9, (November 2005)

Two dimensional simulation of ion beam-plasm interaction

***I. M. Echi**
Department of Physics, University of Ibadan,
Ibadan, Nigeria
and
R. Akin-Ojo
Department of Physics, University of Ibadan,
Ibadan, Nigeria

Abstract

Hybrid plasma simulation is a model in which different components of the plasma are treated differently. In this work the ions are treated as particles while the electrons are treated as a neutralizing background fluid through which electric signals may propagate. Deuterium ion beams incident on the tritium plasma interact with the plasma through the wake electric and magnetic fields of the beam currents. The model is described by the Vlasov-Maxwell-fluid equations with displacement currents omitted in the Ampere's equation. Euler scheme advances the ion positions and velocities while finite difference scheme approximates the spatial derivatives of field quantities. Bilinear interpolation is used in interpolating field quantities from the grid points to push particles in their respective positions. The beam parameters that determine the response of the plasma are the beam velocity V_b, the density n_b and the radius r_b. It was found that the sharpness of the characteristic frequencies for power absorption increased with increasing beam density while increasing the beam radius destroyed the characteristic frequencies and spread the frequency band of the continuous lines. The Joule heating of the plasma fluctuated in time and could be localized. Increasing n_b delocalized the heating. The magnetic field profile did not respond sharply to beam parameters but the respond was sufficient enough to cause inhomogeneity in the direction of applied magnetic field B_o.

Keywords*:* Hybrid model, Vlasov-Maxwell, Joule heating, beam-plasma ,beam-density

pp 561 - 572

1.0 Introduction

Many schemes have been proposed for the heating of magnetized plasma for the controlled thermonuclear reaction. The few most intensively researched schemes include the electron and ion cyclotron resonance heating (using radio frequency waves *rf*), ultra relativistic electron beam injection, neutral beam injection, and Ohmic heating (Dovell and Gresillon 1975 [5], Thode 1976 [15], Breun and Ferron 1979 [2]). The neutral beam injection method is collisional and because of charge neutrality there is a relative easy of beam penetration into the plasma. The *rf* heating can be treated at two levels. In one level, one may neglect interaction between plasma particles themselves

*All correspondence to: I. M. Echi, Department of Physics, University of Agriculture, P.M.B 2373, Makurdi, Nigeria, e-mail: idugbaechi@yahoo.com

and consider only plasma-wave interaction. In this simplified form the particle evolution are not coupled to the Maxwell field equations (Karny, 1978 [10]). In the second level, interaction among the plasma particles is allowed in addition to external waves. In either of the two approaches a complete analytical treatment is difficult because of the non-linearity in the particle evolution equation and the complexity in the dielectric permittivity tensor ε, which becomes a functional of the electric field and the particle distribution function. But the power absorption by the plasma due to trapped and untrapped Landau damping is associated with the imaginary part of the longitudinal component of ε while that due to cyclotron resonance is associated with the imaginary part of the transverse component of ε (Kommoshvili et al. 2003 [11]). The way out of these difficulties is to avoid the kinetic dielectric permittivity tensor, and in its place use the cold plasma permittivity tensor (Grishanov et al. 2002 [9]). The cold plasma approximation cannot explain the high frequency phenomena associated with rf heating but it can explain Alfven heating based on mode conversion often called local Alfven resonance (Elfimov and Galvao 2002 [6]).

Computer simulation has become an alternative method of circumventing analytic difficulties in getting insight into the plasma response to any proposed interaction. There is however a problem associated with scale lengths in plasma simulation. The plasma electrons respond to high frequency interactions while the ions to low frequencies. The heat acquired by electrons in high frequency interaction is not available to the ions but it is the ions that have to under go fusion. High frequency simulation thus requires extraneous mechanism for downloading the electron energy into the ions if the aim is to heat the ions. To treat high frequency response, it suffices to assume that the ions are heavy compared with electrons, and constitute fixed positive neutralizing background for the electrons.

In other to treat low frequency phenomena associated with the ions, we need a careful assumption that will make us neglect the displacement currents (responsible for high frequency phenomena) in the Maxwell equations. This is known as Darwin approximation (Matthews 1994, Bagdonat and Motschmann 2002 [1]). The electrons are treated as a fluid through which the ions (particles) move. This is the basis of hybrid simulation.

In this paper we considered a beam of deuterium ions (rather than neutral beams) injected into magnetized tritium plasma. The experimental method by which such a beam may be obtained is described elsewhere (Thode 1976 [15], Toshitaka and Naoyoshi 1985 [16]. The beam is non-relativistic so that collisional mechanisms are not the method by which the beam interacts with the plasma. Rather the beam interacts with the plasma through the wake electric and magnetic fields of the beam currents. The rest of the paper is organized as follows: section 2 gives the theoretical and computational procedure; section 3 treats results and discussion while conclusion is in section 4.

2.0 **Theory of the model and computational procedure**

The hybrid plasma may be described by a combination of Vlasov kinetic equation, the system of Maxwell equations, the fluid equation and Newton's equation as given below (Fruchtman and Weitzner 1986 [8])

$$\frac{\partial f}{\partial t}+(v.\nabla)f+\frac{q}{m}(E+E_b+.\frac{v\times(B+B_b)}{c}).\frac{\partial f}{\partial v}=0 \qquad (2.1$$

$$\frac{\partial \mathrm{B}}{\partial \mathrm{t}}=-\nabla\times E \qquad (2.2)$$

$$\nabla\times \mathrm{B}=\mu_o \mathrm{J}+\frac{1}{\mathrm{c}}\frac{\partial \mathrm{E}}{\partial \mathrm{t}} \qquad (2.3)$$

$$\nabla.\mathrm{E}=4\pi\rho \qquad (2.4)$$

$$\nabla.B = 0 \tag{2.5}$$

$$n_e m_e \frac{du_e}{dt} = -n_e eE + J_e \times B - \nabla P \tag{2.6}$$

$$P_e = n_e kT_e \tag{2.7}$$

$$\frac{dX}{dt} = V \tag{2.8}$$

$$\frac{dV}{dt} = \frac{q}{m}\left(E + V \times B\right) \tag{2.9}$$

Equation (2.1) is the Vlasov equation giving the total time derivative of the particle distribution f in phase space described by the coordinates (*t, r,v*). In the absence of collisions between particles the equation says that the distribution function is constant along the characteristics given by the Newton equations (2.8) and (2.9). The electric field *E* and magnetic field *B* arising from particle motion or applied fields must satisfy the Maxwell equations (2.2 – 2.5). Equation (2.6) is the momentum equation for the electron fluid motion while equation (2.7) gives the pressure exerted by the fluid. In equations (2.1 – 2.9), the symbols not yet defined as follows: q is ion charge, μ_o is the permeability of free space, *J* is total current density, ρ is charge density, n_e is electron number density, m_e is electron mass, v is the ion velocity, *k* is Boltzmann constant and P_e is the electron pressure. We considered a non-relativistic deuterium beam that is Gaussian in both transverse coordinates (*x,y*). The electric $E_{b,}$ and magnetic B_b fields of the beam current are given by

$$E_b = \frac{qn}{2\pi\varepsilon_o r}(1 - e^{-r^2/2a_o{}^2}) \tag{2.10}$$

$$B_b = \frac{\mu_o qnv}{2\pi r}(1 - e^{-r^2/2a^2 o}) \tag{2.11}$$

where $r = (x^2 + y^2)^{1/2}$,v_b = beam velocity and a_o is arbitrary (taken as fraction of scale length of the system). We assumed the plasma is quasi-neutral, implying that the total electron charge density is equal to the ionic charge density, i.e.

$$n_e e = \rho_i \tag{2.12}$$

where ρ_i is ionic charge density. The displacement currents in the Ampere's law equation (2.3) is neglected (Darwin approximation). By this assumption there is no explicit time evolution for the electric field. The electric field is determined by rearranging equation (2.2) and (2.6) to give

$$E = -\frac{J_i \times B}{\rho_i} + \frac{(\nabla \times B)\times B}{\mu_o \rho_i} - \nabla P \tag{2.13}$$

where we have used the fact that the total current *J* is the sum of the ionic J_i and electronic J_e currents (J_e = *neu*, *u* = electron fluid velocity), and that the electron fluid is massless (hence $nm_e du/dt = 0$). The magnetic field evolution equation (2.2) can thus be written as

$$\frac{\partial B}{\partial t} = \nabla \times \frac{J_i \times B}{\rho_i} - \nabla \times \frac{(\nabla \times B)\times B}{\mu_o \rho_i} \tag{2.14}$$

Finally, we assumed that the electron fluid pressure is uniform in space, thus ∇P = 0 in equation (2.13) and is omitted in equation (2.14). Equations (2.8 – 2.14) are the simplified hybrid model equations. They are all vector equations that have to be decomposed into components. For example, the x-component of the magnetic evolution is of the form

$$\frac{dB_1}{dt} = \frac{d}{dy}(J_1B_2 - J_2B_1)/\rho_i - \frac{d}{dy}(B_2\frac{dB_3}{dy} + B_1\frac{dB_3}{dx})/\mu_o\rho_i \qquad (2.15)$$

Spatial derivatives were approximated by finite differences in a rectangular grid. The rectangular plane of size (L_x,L_y) = (10cm, 10cm) was divided into cells of size (dx,dy). The magnetic field B, the current density J_i and the charge density ρ_i were evaluated at full integer grid points ($n_1$dx, n_2dy), $n_{1,2}$ = 1, 2,---. The electric field E, was placed on an interlaced grid with nodes at $(n_1 + 1/2)dx$, $(n_2 + 1/2)dy$ because its curl was required to evaluate dB/dt. Charged particles within $i - 1/2 - i + 1/2$, $j - 1/2 - j + 1/2$ were binned to the node $N_{ij}(i, j = 1, 2,---)$. The total charge at a particular grid (the macro particle charge) was not just the sum of all the particle charges binned to the point but a weighted sum reflecting the position of each particle from the grid node. For example, a particle in a position r_k contributes to the macro-particle charge of the grid node an amount $\bar{q} = \frac{qr_k}{r_g}$, where r_g is the grid size. Since the model is 2-D, this weighting is an area weighting.

The field quantities B and E were defined only at the grid nodes but the particles occupied positions all around the nodes. The field felt by a particle j binned to a grid node n_{ik} was estimated by a bilinear interpolation using field values from the four nearest nodes containing the particles (Press et al. 1986 [13]), i.e.

$$\Psi(x,y) = (1-t)(1-u)\Psi_{i,k} + t(1-u)\Psi_{i+1,k} + tu\Psi_{i+1,k+1} + (1-t)u\Psi_{i,k+1} \qquad (2.16)$$

where, $t = \frac{x-x_i}{\Delta x}, u = \frac{y-y_k}{\Delta y}$, and ψ is the field E or B.

The tritium ions were pushed by the mid-point scheme

$$X^{1/2} = X^{-1/2} + V^o dt, V^1 = V^o + \frac{q}{m}[E^{1/2}(X^{1/2}) + V^{1/2} \times B^{1/2}(X^{1/2})]dt \qquad (2.17)$$

where,
$$V^{1/2} = V^o + \frac{q}{m} dt[E^{1/2} + V^o \times B^{1/2}], \qquad (2.18)$$

$X \equiv (x,y)$, and the superscripts refer to time levels. The particle positions and their velocities leap-froged over each other. The leap-frog scheme introduces a free streaming current density J^* (particle velocities remaining constant while positions changed). The total current density at half-time step $J^{1/2}$ was computed as the sum of J^+ and the contribution from E^* and $B^{1/2}$

$$J^{1/2} = J^* + \frac{dt}{2}(\beta E^* + \alpha \times B^{1/2}) \qquad (2.20)$$

where

$\beta = \sum_s G(X^{1/2}){q_s}^2/m_s, \alpha = \sum_s G(X^{1/2}){q_s}^2 V^o/m_s$, $E^* = E(\rho^{1/2}, J^o, B^{1/2})$ and

G is area weighting factor (s = 1 for one specie plasma).

We did not follow the deuterium beam dynamics. The beam only provided the wake fields that interact with the tritium plasma.

A total of 2000 tritium ions, 1000 - 4000 deuterium ion beam were used in the simulation. A random function (from the system random generator) generated a set of particle positions X and their corresponding velocities in the interval X, $V \in [0.1]$. An amplification factor AP = 100 spread the random sets to cover the simulation space. Starting with the set $X^{1/2}$, v^o, B^o the computational cycle proceeded as shown in the flow chart below.

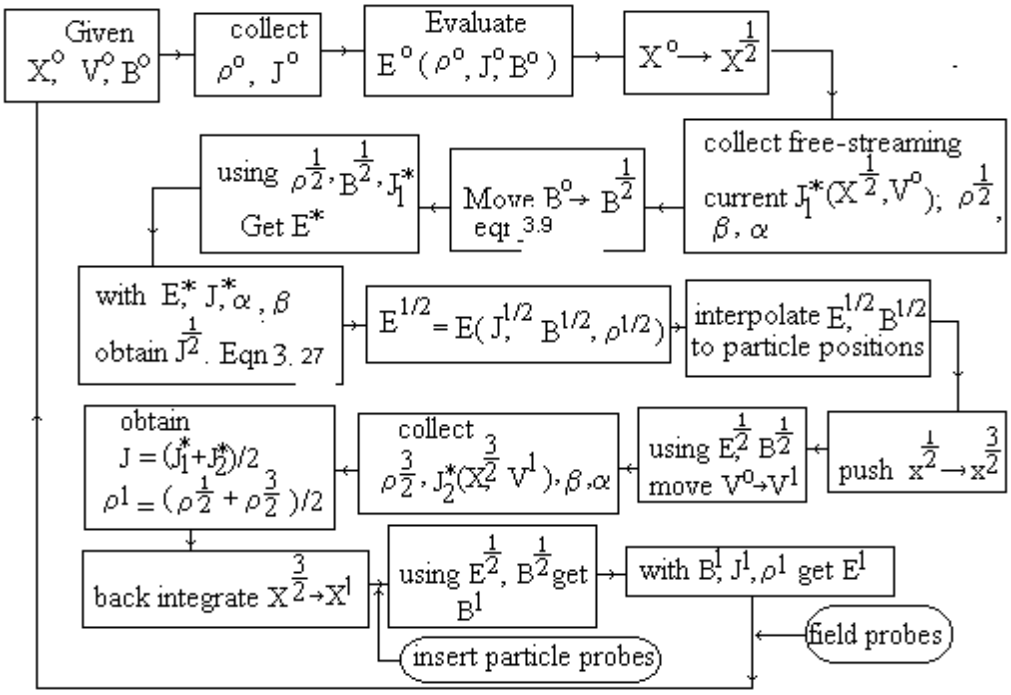

Figure 1: Block diagram of the computational procedure.

The code is well structured such that the evaluation of any quantity in the box is by means of a call to appropriate subroutine. For example, in one computational cycle the subroutine PUSH will be called twice to push particles from $X^o \rightarrow X^{1/2} \rightarrow X^{2/3}$. The subroutine CHARGE will be called three times corresponding to time levels 0, ½ , 2/3. The primary data outputs are those of particle positions, velocities, the electric and magnetic fields at the end of a cycle. Every diagnostics must be in terms of the primary data. In this paper we report the measurements of the power spectrum of the electric field, particle diffusion, charge density fluctuation and Joule heating of the plasma. Each of these quantities has appropriate subroutine that draws appropriate data and evaluates the quantity.

The power spectrum of the electric field was computed by first taking the autocorrelation $G(\tau)$ of the electric field and then the cosine transform of the autocorrelation (Dawson 1983 [3], Press 1983 [13]),

that is, $$G(\tau) = \frac{1}{T}\int_0^t E(t)E(t+\tau)dt \qquad (2.21)$$

$$P(\omega) = \int G(\tau)\cos(\omega\tau)d\tau \qquad (2.22)$$

The Joule heating $H(X,t)$ was estimated as the product of the current density J and the electric field E;

$$H(X,t) = J.E \qquad (2.23)$$

Constants such as electron charge, proton mass, magnetic permeability, electric permittivity of free space, ambient magnetic field B_a, Alfven wave velocity V_A were assigned arbitrary simulation values. This is often the practice in simulation since the essence is to get an insight about the nature of the response of the system to the perturbations rather than actual values.

3.0 **Results and discussion**

Figure 1a shows the power spectrum of the background electric field, that is, when there is no beam. There is a pick about zero frequency and a continuous spectrum. The total energy (numerically equal to the area under the curve) available in the wave frame is very small. The power axis is of the

order of $10^{-4}Js^{-1}$. When the deuterium ion beam with parameters $V = 0.2V_A$, $n_b = 0.5n_p$ and radius $r_b = 1.2a_o$ is switched on, four characteristic frequencies for energy absorption can be seen on the spectrum (Figure 1b). The characteristic frequencies become very sharp when the beam density is increased to $n_b=2n_p$ (Figure 1c). The total energy available in the wave frame is very large compared to when there were no waves. The sharpness of the characteristic frequencies is found to increase with increasing beam density keeping other beam parameters constant. However, the increasing the beam radius from $r_b = 1.2a_o$ to $r_b = 1.5a_o$ destroys two of the characteristic lines and spread the frequency of the continuous spectrum (Figure 1d). Higher and higher beam radius eliminates characteristic lines suggesting that narrow deuterium ion beams excite waves of characteristic frequencies than a broad beam. This is consistent with equation (10) and equation (11) which show that the beam electric and magnetic fields are stronger for a narrow beam than a broad one, Similarly, beams of higher density give stronger electric and magnetic fields than low density beams. When the beam fields are strong, they couple more effectively with the plasma giving rise to wave excitations at multiple frequencies.

The magnetic field profile did not oscillate like the electric field. It either grows or falls continuously as shown in Figure 2 for the *z*-component in the core region of the plasma. The profile of B_3 (*z*-component) shows that the applied constant magnetic field B_o is well influenced by the electric and magnetic fields of the beam and plasma currents. The influenced is not uniform across the plasma. Close to the edge (region 2,2) of the plasma B_3 is enhanced while at the core, region (5,5) it is degraded (Figures. 2a and 2b). The beam plasma interaction has thus introduced inhomogeneity in the confining magnetic field B_o. The plasma ion drift velocity will respond to this inhomogeneity and subsequently the electric field. This may probably be the cause of localized heating and turbulence reported by Ferreira et al (2002) [7]. Surprisingly, the magnetic field evolution appears not to respond to changing beam data.

Figure 3 shows the macroparticle charge density fluctuation with time in the core region of the plasma. The beam parameters are $V_b = 0.2V_A$, $n_b = 0.5n_p$ and $r_b = 1.2a_o$. The fluctuation of the charge density is expected as the plasma ions feel different forces depending on their positions and velocities. The fluctuation however, is always positive as it should be otherwise the electric and magnetic field of the excited waves will be infinite (equations. 2.13 and 2.14). The charge density fluctuations are similar for other beam-plasma parameters. This is expected since periodic boundary conditions ensure that the plasma particles are conserved within the simulation plane.

Figure 4 shows the rate of Joule heating of the plasma. When there is no beam, no appreciable heating takes place for a very long time and when it started it rather drain energy from the plasma. This is perhaps due to wave excitation, which in the absence of beams may have occurred at the expense of the plasma internal energy (Figure 4a). When the beam parameters are $V_b = 0.2V_A$, $n_b = 0.5n_p$ and $r_b = 1.2a_o$, the core region of the plasma becomes heated almost immediately the beams enter the plasma (Figure 2.4a and 2.4b). Near the boundary no heating takes place for a long time (Figure 2.4c). It is most probable that the core heats first and thereafter convection through the electron fluid takes the heat to the boundary. When the beam density is increased such that $n_b = n_p$, both the core and the edge heat almost immediately though the core cools faster than the edge. The beam density $n_b = 2n_p$ makes the core and the boundary regions to heat continuously. When the beam radius is increased from $1.2a_o$ to $2.5a_a$ it was found that the direction of the convection has reversed in that the boundary region heats faster than the core. Since the Joule heating is proportional to the product of J and E, either or both may affect the heating rate. However, since the charge density is nowhere zero, the current density too will be nowhere zero. The vanishing or localized Joule heating must be attributed the electric field of waves.

Other common diagnostics of plasma simulation include the electric field profile, the particle distribution, the drag on particles and diffusion. The effect of beam parameters and the quiet initialization mode on these quantities shall form the subject of our next report.

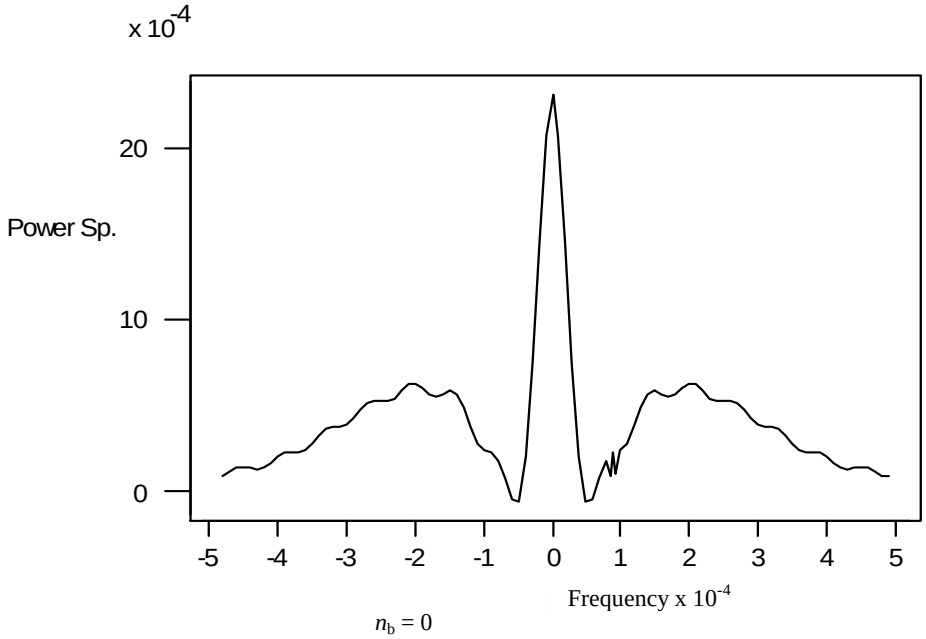

$n_b = 0$

Figure 1(a): Power spectrum of the electric field.

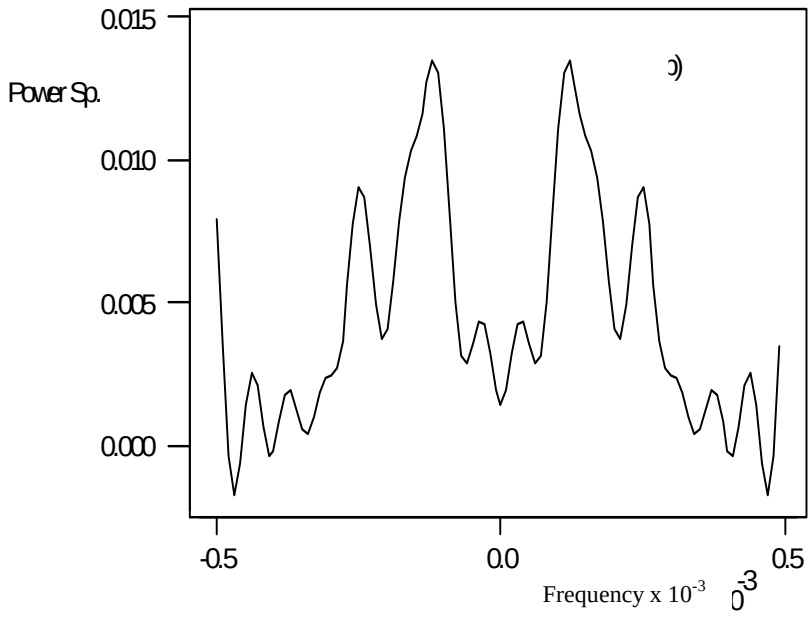

$v_h = 0.2v_A$, $n_h = 0.5n_n$, $r_h = 1.2a_o$

Figure 1(b): Power spectrum of the electric field

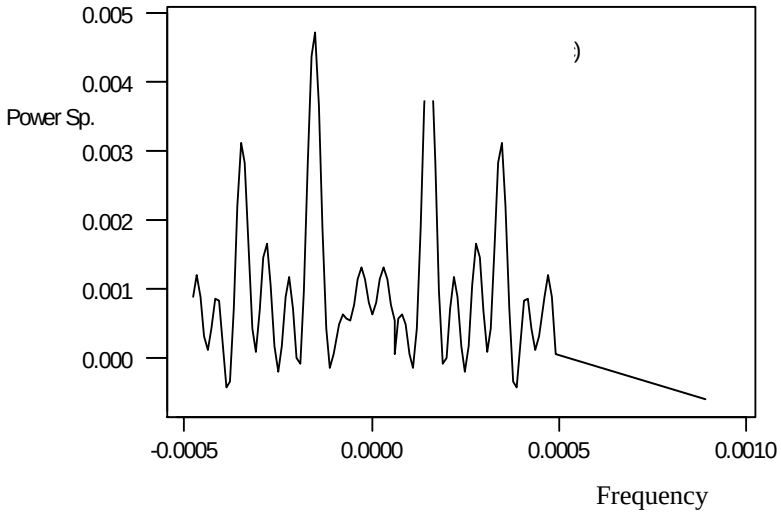

$v_b = 0.2v_A$, $n_b = 2n_p$, $r_b = 1.2a_o$

Figure 1(c): Power spectrum of the electric field

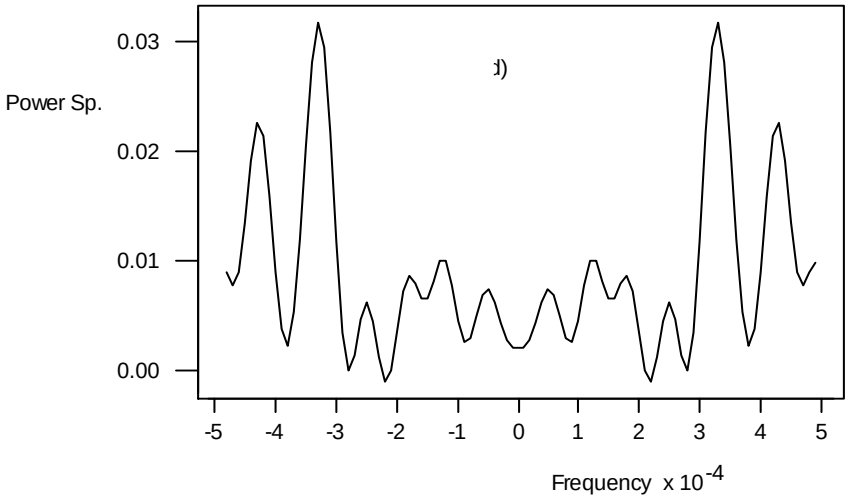

$v_b = 0.2v_A$, $n_b = 2n_p$, $r_b = 1.5a_o$

Figure 1(d): Power spectrum of the electric field

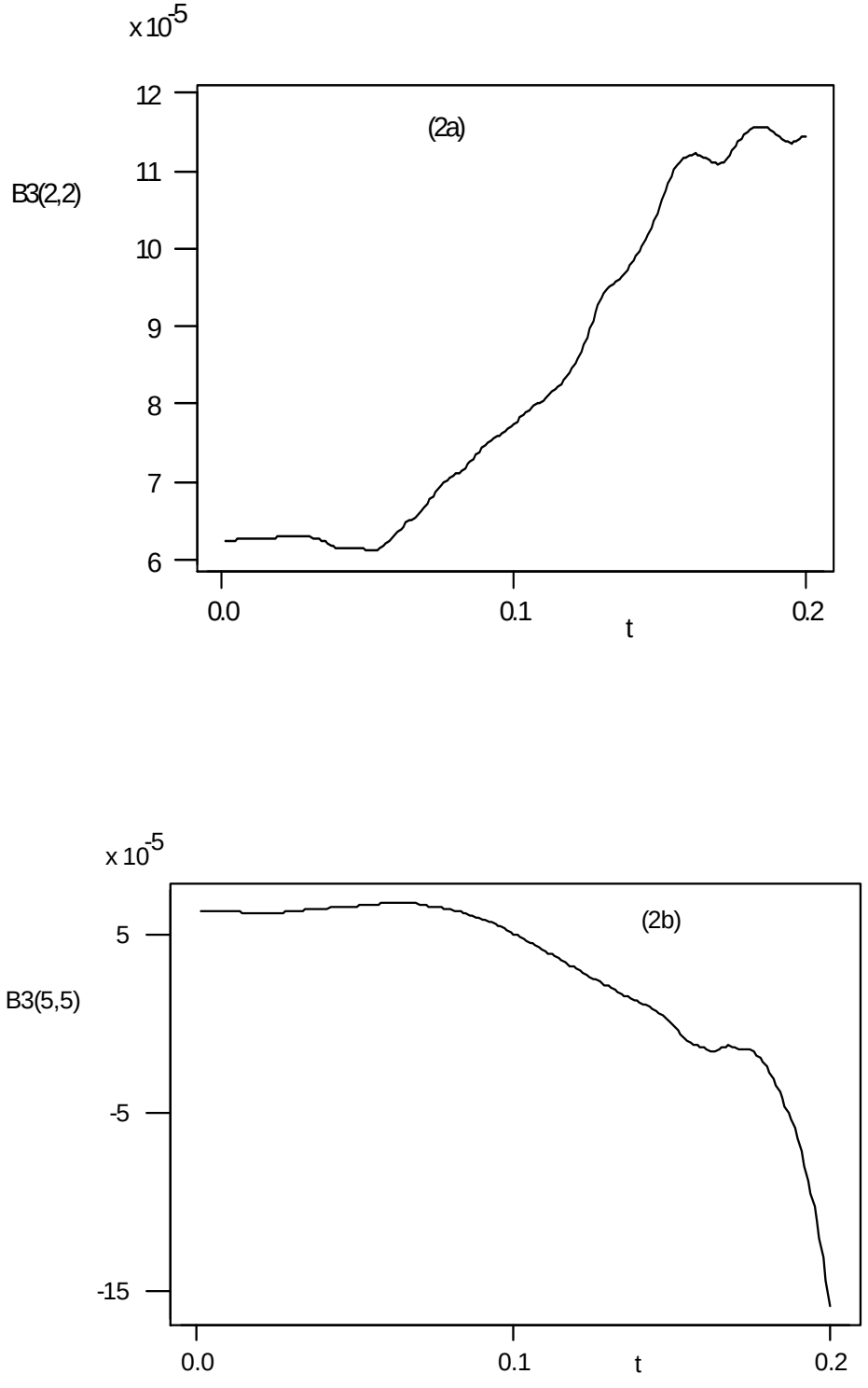

Figure 2: Z-component of the magnetic field profile (a) near the edge, (b) at the core

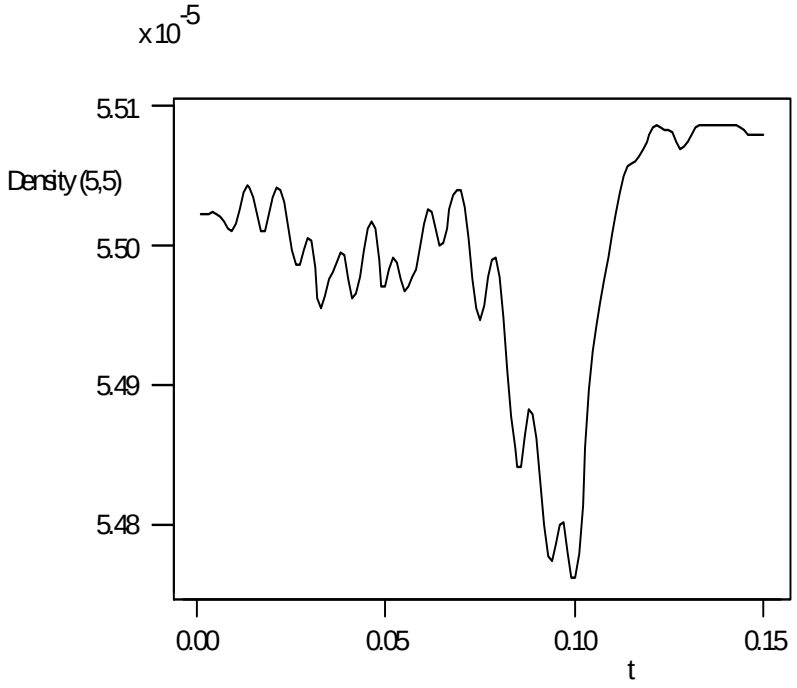

Figure 3: Charge density profile at the core

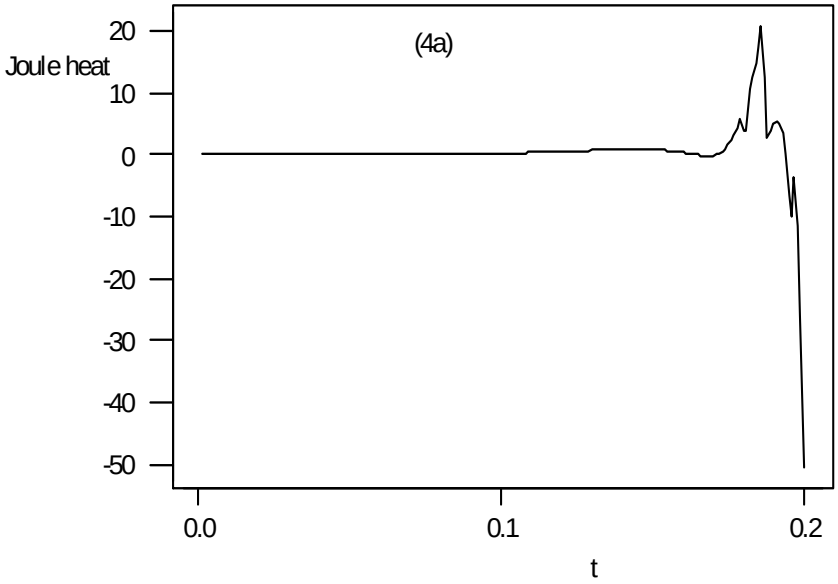

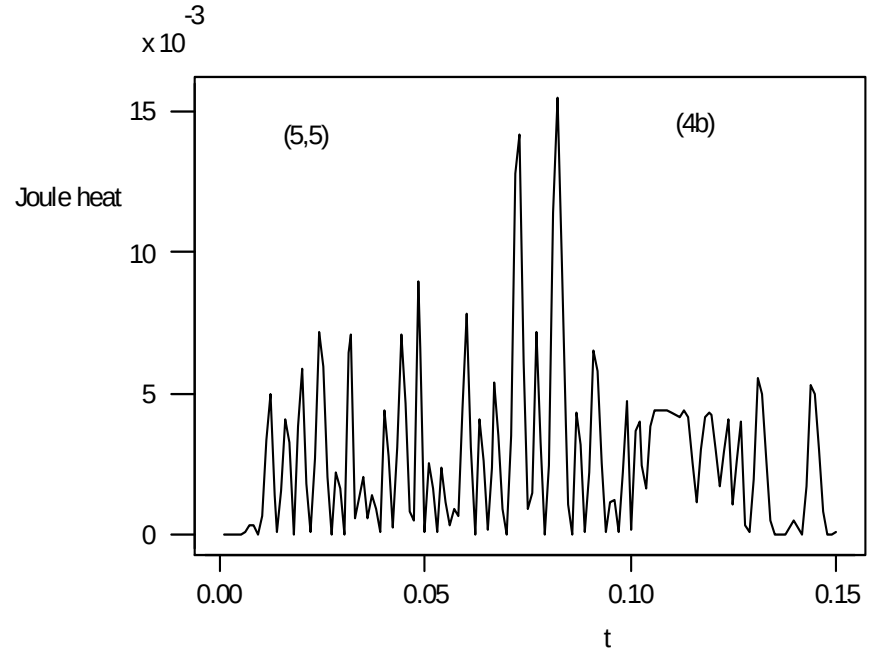

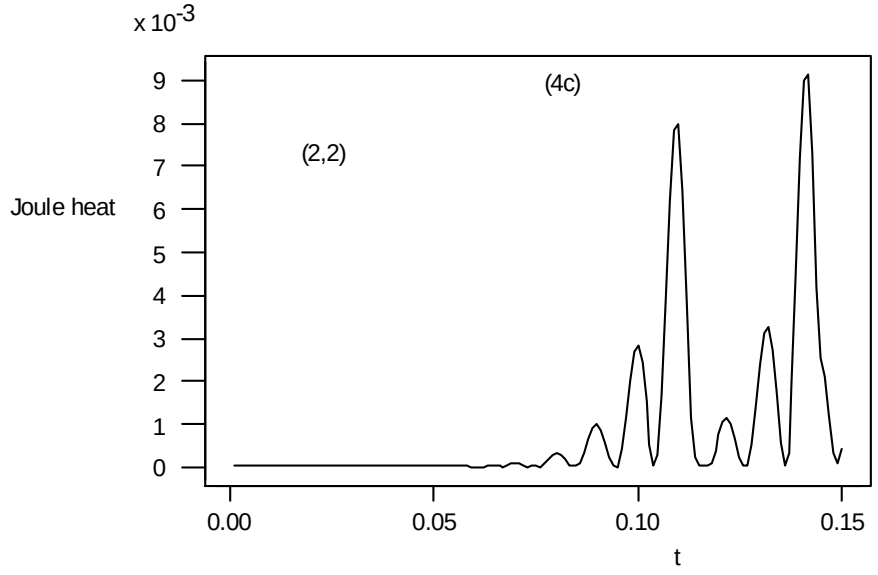

Figure 4: Joule heating as a function of time (a) no beam, (b) core region, (c) near the edge; in a and b: $v_b = 0.2v_A$, $n_b = 0.5n_p$, $r_b = 1.2a_o$

4.0 Conclusion

We have successfully simulated the hybrid model of beam plasma interaction using our code. It was found that for a fixed beam radius r_b and velocity v_b, plasma heating is more effective when a dense ion beam is used than a sparse one. Similarly, for fixed beam parameters, plasma heating is higher with a narrow beam than a broad one. The Joule heating is very sensitive to the beam parameters. The heating may be localized, continuous or zero, depending on the beam data. Convection effects through the electron fluid serve to distribute the localized heating. Unlike the power spectrum and Joule heating, the magnetic field profile is not sensitive to the beam parameters but it is sufficient enough to cause modification of the applied magnetic field B_o. The charge density fluctuation is everywhere positive definite within the simulation space therefore ensuring that the electric and magnetic fields of the excited waves remain finite.

References

[1] Bagdonat T and Motschmann U (2002). Hybrid simulation code using curvilinear coordinates. Journal of computational Physics 183, 2, 470-485.

[2] Breun R.A and Ferron J.R (1979). Fast ion beam-plasma interaction. Review of Scientic Instrument 50, 7, 862-866.

[3] Dawson J.M (1983). Particle simulation of plasma. Rev. of Mod. Phys. 55,2,403-447.

[4] O Z (1998). Hybrid model of a rectangular hallow cathode discharge. Physical Review E, 58,6,7126-7137.

[5] ll F and Gresillon D (1975). Space-time structure of ion beam-plasma turbulence. Physics of fluids 18,12,1756-1762

[6] Elfimov A.G and Galvao R.M (2002). Calculations of Alfven wave heating in TCABR Tokamak. Brazilian Journal of Physics. 32,1,34-38.

[7] Ferreira A.A, Heller M.V, Baptista M.S and Caldas I.L (2002). Statistics of turbulence induced by magnetic field. Brazilian Journal of Physics 32,1,85-88.

[8] Fruchtman A and Weitzner H (1986). Fundamental ion-cyclotron frequency heating in tokamaks. Phys. Fluids 29,12,4261-4173.

[9] Grishnov N.I, Azevedo C.A and Neto J.P (2002). Collisionless dissipation of radio-frequency waves in axiymmetric Tokamak plasma. Brazilian Journal of Physics, 32,1,179-186.

[10] Karney C.F.F (1978). Stochastic ion heating by lower hybrid wave. Phys. Fluids 21,9,2188-2209.

[11] Kommoshvili K, Cuperman S, Bruma C (2003). Kinetic effects in the conversion of fast waves in pre-heated, low aspect ratio tokamak plasma. Plasma Phys. Control Fusion 45,275-287.

[12] Matthew A.P (1994). Current Advance method and Cyclic Leapfrog 2D Multispecies Hybrid plasma simulations. Journ. Comp. Phys. 112,102-116.

[13] Press W.H, Teukolsky,Vetterling W.T and Flannery B.P (1986).Numerical Recipes in Fortran. Cambridge Uni-press, England, 2nd Edition

[14] Riyopoulos S and Tajima T (1986). Simulation study of two-ion hybrid resonance heating.Phys. Fluids, 29,12,4161-4173.

[15] Thode L.E (1976). Plasma heating by scattered relativistic electron beams: correlations among experiment, simulation and theory. Physics of fluids 19,6,831-848

[16] Toshitaka I and Naoyoshi T (1985). Instability near the lower-hybrid frequency in an ion beam-plasma system. Phys. Fluids 29,4,1089-1092.